The Bangudae Petroglyph in Ulsan, Korea: studies on weathering damage and risk prognosis

B. Fitzner · K. Heinrichs · D. La Bouchardiere

Abstract The prehistoric Bangudae Petroglyph in the Ulsan area represents an outstanding National Treasure of the Republic of Korea. Since the construction of the Sayeon dam, the petroglyph with about two hundred carvings is periodically submerged by the Sayeon reservoir. The danger of increasing damage has resulted in intensive efforts to protect this cultural heritage. Diagnosis and risk prognosis studies were carried out. Results of petrographical studies, monument mapping and in situ measurements are presented. Types, degree and zonation of damage are evaluated. The risk estimation derived from the studies confirms the necessity of preservation measures.

Keywords Petroglyph · Rock weathering · Damage diagnosis · Risk estimation · Republic of Korea · Ulsan Metropolitan City · Daegok-Ri

Introduction

Petroglyphs are known as the world's oldest examples of rock sculpture. They are of high archaeological value and they represent very important cultural heritage. The Bangudae Petroglyph in the area of Ulsan Metropolitan City in the southeastern part of the Republic of Korea is considered to be a prominent masterpiece of prehistoric rock carving. The petroglyph—about 10 m wide and 3 m high—was carved in a period between the end of the Neolithic Age and the Bronze Age. In 1971 the Bangudae Petroglyph was rediscovered, and in 1995 it was designated Korean National Treasure (No. 285). The petroglyph shows about 200 carvings including land animals, sea animals and hunting scenes (Figs. 1, 2, 3, 4). The carving techniques are classified into Myeonjjogi—chiselling out completely the inside of the object, and Seonjjogi—chiselling just outlines. The petroglyph was carved on a cliff, which is composed of sedimentary rocks—sandstone, siltstone, sandy shale—of the Silla Series/Cretaceous. The bedding planes incline with 12.5° in direction of NW. The cliff is affected by a considerable number of structural discontinuities. The petroglyph is protected against rain by protruding rocks above it.

The Bangudae Petroglyph is situated at the Daegok River, a tributary of the Taehwa River (Fig. 5). In the period between 1962 and 1965, the Sayeon dam was built on the Daegok River establishing a water resource for Ulsan Metropolitan City. Since the construction of the dam, the Bangudae Petroglyph is submerged for about 8 months/year—from early spring to autumn—by the Sayeon reservoir (Fig. 6). The consequent danger of increasing stone deterioration and, thus, irretrievable loss of most important cultural heritage, has resulted in intensive efforts to prevent damage and to protect the petroglyph for future generations.

In 2002, the International Symposium on the Conservation of the Bangudae Petroglyph took place in Ulsan as a forum for discussing appropriate approaches (Kim 2002). On behalf of Ulsan Metropolitan City, the working group "Natural stones and weathering" of the Geological Institute—RWTH Aachen University/Germany carried out studies on the Bangudae Petroglyph. The studies combined laboratory analyses of representative stone samples and investigation on site. The evaluation and scientific rating of the weathering damage on the Bangudae Petroglyph, the petrographical characterization of the rocks, a risk prognosis and the deduction of information on need and urgency of preservation measures were the overall aims of these studies.

Received: 20 July 2003 / Accepted: 20 January 2004
Published online: 4 May 2004

B. Fitzner (✉) · K. Heinrichs · D. La Bouchardiere
Geological Institute, RWTH Aachen University,
Wuellnerstraße 2, 52062 Aachen, Germany
E-mail: fitzner@geol.rwth-aachen.de
Tel.: +49-241-8095727
Fax: +49-241-8092346

Methods

The investigation areas at the Bangudae Petroglyph are presented in Fig. 7. Five stone samples were collected from non-carved areas of the petroglyph for petrographical study. The numbering of the samples from Bangudae 1 to Bangudae 5 correlates with the locations of sampling from

 DOI 10.1007/s00254-004-1052-x

Fig. 1
Model of the Bangudae Petroglyph

bottom to top of the investigation area. Stone properties such as macroscopic characteristics, mineral composition, microtexture/-structure, porosity properties, hygric properties and petrophysical properties were studied by means of macroscopic description, binocular microscopy, X-ray diffraction analysis, transmitted light microscopy with image analysis, scanning electron microscopy, mercury porosimetry, nitrogen adsorption method (BET), water absorption/desorption tests and ultrasonic measurements. Exemplarily, differences between unweathered and weathered stone were lined out for one sample (Bangudae 2).

The investigation of the Bangudae Petroglyph comprised monument mapping—in particular the mapping of weathering forms—and systematic non-destructive measurements such as ultrasonic measurements, rebound hardness measurements and profile measurements. The monument mapping method was applied as a non-destructive procedure for the precise evaluation and rating of the weathering damage on the petroglyph.
Weathering forms are used for the precise description of deterioration phenomena at centimetre to metre scale. They represent the visible result of weathering processes that are initiated and controlled by interacting weathering factors. By means of weathering forms, the weathering state of stone surfaces are described according to phenomenological/geometrical criteria. The objective and

Fig. 2
Carving

Fig. 3
Carving

Fig. 4
Carving

reproducible registration of weathering forms requires a detailed classification scheme of weathering forms. Such a standard classification scheme was developed based on investigation of stone monuments worldwide considering different stone types and environments (Fitzner and others 1995; Fitzner and Heinrichs 2002).
As the result of a systematic survey of weathering forms on the Bangudae Petroglyph, this classification scheme was tailored to optimal applicability at the petroglyph. The optimization has included a suitable intensity classification of the weathering forms. Based on this classification scheme, the mapping method was applied for the detailed registration, documentation and evaluation of the weathering forms. Large-sized photographs of the petroglyph were used as documents for the mapping of weathering forms and for the preparation of plans. The weathering forms were illustrated in maps and were evaluated quantitatively. Damage categories and a damage index were used for the rating of the weathering forms (Fitzner and Heinrichs 2002; Fitzner and others 2002).
Systematic non-destructive measurements were carried out on site in order to obtain supplementary information for the characterization of the rocks and carvings and their state of deterioration.
Ultrasonic measurements were executed with a STEINKAMP Ultrasonic Tester BPV (conic probes, 50 kHz) according to the refraction mode, which means that pulse sender and receiver are positioned on the same side of a stone object. A rectangular grid of almost two hundred measuring points was arranged on the stone surface. The horizontal and vertical distance between adjacent measuring points amounted to 30 cm. Measurements were made along horizontal, vertical and diagonal measuring distances. The evaluation of results included the determination of ultrasonic velocities from measuring distance and transit time and the illustration of the ultrasonic velocities in a map by means of isolines. The distribution of the ultrasonic velocities was classified.
Rebound hardness measurements were made with a Schmidt hammer (PROCEQ LR, impact energy: 0.735 N·m) using the same grid of measuring points as for the ultrasonic measurements. Test measurements on bedrocks near the petroglyph had shown that the procedure does not harm the rocks. The rebound hardness (numerical value, no unit of measure) represents a suitable parameter for rock characterization and the quantification of stone deterioration, especially with respect to disintegration/detachment of stone material. The evaluation of results comprised the classification of rebound hardnesses and the evaluation of rebound hardnesses comparing non-carved and carved areas and considering different weathering forms.
Results obtained from monument mapping and measurements (ultrasonic measurements, rebound hardness

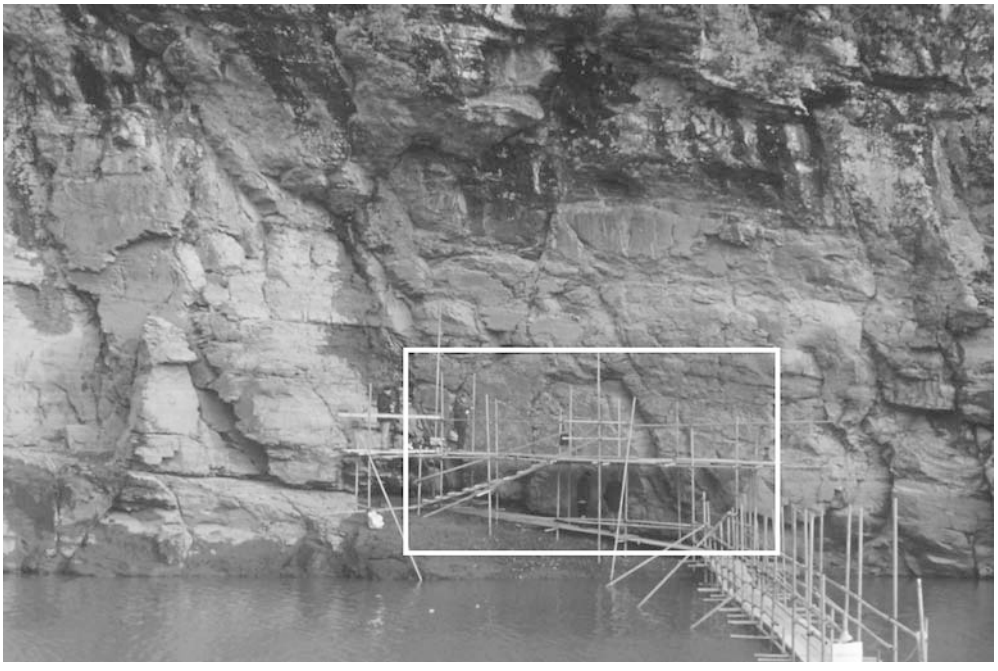

Fig. 5
The Bangudae Petroglyph (*white-framed*) at the Daegok River

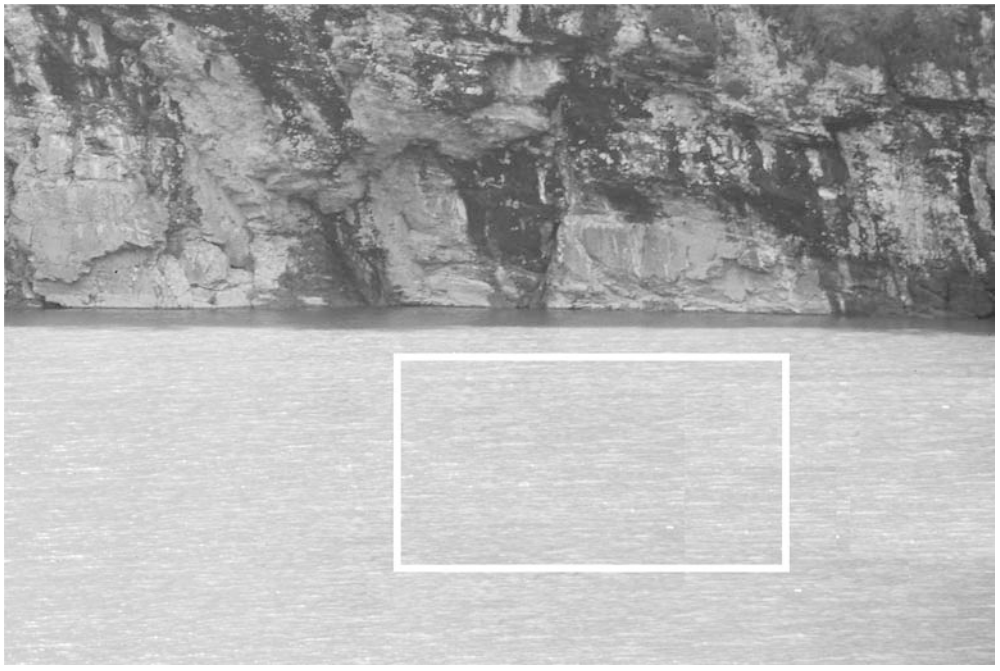

Fig. 6
The Bangudae Petroglyph (location indicated by the *white frame*) submerged by the Sayeon reservoir water

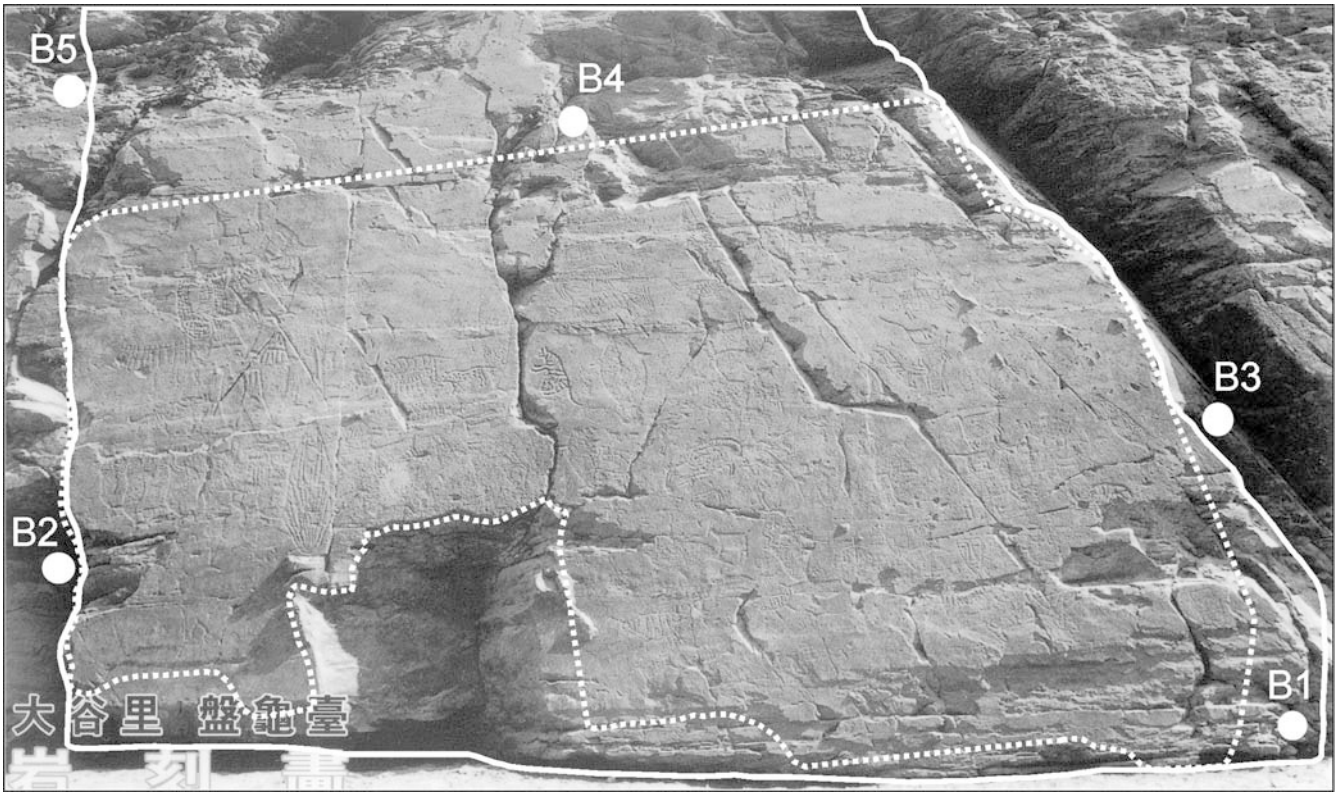

Fig. 7
Investigation areas—monument mapping (*white contour line*), in situ measurements (*white dashed contour line*). Locations of sampling— samples Bangudae 1–5

measurements) were combined for the characterization and quantification of damage zonation at the Bangudae Petroglyph.

Profile measurements with a profile comb were carried out at 40 carvings in order to quantify the morphological profile of the carvings. The length of the measuring sections was 15 cm. The evaluation of results included the graphic documentation of the profiles, the determination of maximum and average depths and the deduction of a quantitative risk prognosis.

Table 1
Petrographical properties of the samples Bangudae 1–5

		Bangudae 1	Bangudae 2		Bangudae 3	Bangudae 4	Bangudae 5
			Unweathered	Weathered			
Macroscopic characteristics		Clayish-silty, compact stone; dark reddish grey	Clayish-silty, compact stone; dark reddish grey; laminated	Greyish brown	Clayish-silty, compact stone; dark reddish grey; laminated; rarely fine fissures	Clayish-silty, compact stone; dark reddish grey; laminated; rarely fine fissures	Clayish-silty, compact stone; dark reddish grey; laminated; rarely fine fissures
Mineral composition (%)	Quartz	7.8	7.6	7.4	5.7	4.1	3.2
	Feldspar	14.1	11.3	14.8	8.1	4.8	5.1
	Rock fragments	2.0	1.7	3.5	1.8	10.0	2.9
	Matrix – clay minerals/micrite	64.7	65.4	69.6	76.5	74.1	81.7
	Matrix – sparite	8.4	10.3	0.1	5.3	4.2	4.9
	Matrix – opaque matter	1.8	1.6	1.4	1.1	1.5	1.1
	Mica	0.9	1.2	2.7	1.0	0.9	0.9
	Chlorite	0.2	0.5	0.4	0.3	0.2	0.1
	Heavy minerals	0.1	0.4	0.1	0.2	0.2	0.1
Matrix-grain-relation	Matrix-grain-ratio (–)	2.98	3.41	2.46	4.84	3.95	7.13
	Fabric	Matrix-supported	Matrix-supported		Matrix-supported	Matrix-supported	Matrix-supported
Petrographic classification (according to Pettijohn and others 1987)		Feldspathic greywacke	Mudstone		Mudstone	Mudstone	Mudstone
Grain size characteristics	Mean grain size (μm)	63.8	45.6		43.8	74.8	51.2
	Sorting (–)	1.32 good	1.23 very good/ good		1.20 very good	1.42 moderate	1.26 good
	Grain size distribution, grains >30 μm (%)						
	Coarse silt (31–63 μm)	56.5	82.3		83.7	44.2	73.5
	Very fine sand (63–125 μm)	36.0	17.1		15.0	39.1	23.5
	Fine sand (125–250 μm)	6.3	0.3		–	12.0	1.5
	Medium sand (250–500 μm)	0.6	0.3		1.3	3.5	0.9
	Coarse sand (500–1,000 μm)	0.6	–		–	0.9	0.3
	Very coarse sand (1,000–2,000 μm)	–	–		–	0.3	0.3

Table 2
Petrographical/petrophysical properties of the samples Bangudae 1–5

		Bangudae 1	Bangudae 2		Bangudae 3	Bangudae 4	Bangudae 5
			Unweathered	Weathered			
Porosity properties	Density (g/cm^3)	2.69	2.69	2.67	2.70	2.70	2.70
	Bulk density (g/cm^3)	2.63	2.58	2.19	2.66	2.65	2.66
	Total porosity (vol.-%)	2.3	4.1	18.1	1.8	2.0	1.5
	Porosity – micropores, radii ≤ 0.1 μm (vol.-%)	0.9	1.5	2.2	0.3	0.6	0.6
	Porosity – capillary pores, radii >0.1 μm (vol.-%)	1.4	2.6	15.9	1.5	1.4	0.9
	Pore surface (m^2/ g, *m^2 / cm^3*)	2.7, *7.2*	3.0, *7.7*	5.1, *11.2*	1.8, *4.8*	2.2, *5.9*	2.5, *6.6*
Hygric properties	Water absorption at atmospheric pressure (weight-%, *vol.-%*)	0.75, *2.00*	1.63, *4.16*		0.72, *1.92*	0.60, *1.59*	0.51, *1.37*
	Water absorption at pressure – 150 bar (weight-%, *vol.-%*)	0.77, *2.05*	2.07, *5.27*		0.74, *1.98*	0.68, *1.80*	0.54, *1.45*
	Saturation coefficient	0.97	0.79		0.97	0.88	0.94
	Rest water content after drying -7 days, 20 °C/ 50% rel. humidity (weight-%, *vol.-%*)	0.26, *0.70*	0.42, *1.07*		0.28, *0.75*	0.25, *0.66*	0.24, *0.65*
	Rest water content in relation to maximum water absorption at pressure (%)	34.2	20.3		37.9	36.7	44.5
Petrophysical properties	Ultrasonic velocity parallel to bedding (m/s)	4,376	4,428	3,611	4,314	4,519	4,328
	Ultrasonic velocity perpendicular to bedding (m/s)	4,070	4,239	3,218	3,434	3,610	2,827

Results

The petrographical/petrophysical properties of the five stone samples are presented in the Tables 1and 2. The samples can be described as clayish-silty, compact stones of dark reddish grey colour. The samples Bangudae 1, 4 and 5 show partly a heterogeneously distributed accumulation of coarser grains. The samples Bangudae 2–5 are characterized by a very fine lamination and micro-fissures. The samples Bangudae 1, 2 and 5 show a marginal, greyish-brown weathered zone. The thickness of this weathered zone ranges between 0.2 cm (Bangudae 5) and 1 cm (Bangudae 2). The sample Bangudae 2 was selected for a detailed comparison of unweathered and weathered stone material. The unweathered parts of the samples are composed of quartz, feldspar (albite, microcline), rock fragments, matrix minerals, mica (especially muscovite), chlorite and heavy minerals. The matrix is composed of clay minerals (especially chlorite, muscovite/sericite), carbonate (micritic and sparitic calcite) and opaque matter (hematite). Comparing the samples, the content of quartz and feldspar decreases from Bangudae 1 to Bangudae 5, whereas the proportion of matrix increases. Comparing unweathered and weathered parts of Bangudae 2, the loss of carbonate in the weathered part is the most striking characteristic. According to the petrographical classification scheme of Pettijohn and others (1987), Bangudae 2–5 are mudstones. Bangudae 1 is to be classified as feldspathic greywacke.

In all samples most of the grains are either coarse silt (31–63 μm) or very fine sand (63–125 μm). The mean size of the grains ranges between 43.8 μm (Bangudae 3) and 74.8 μm (Bangudae 4). Correlating with increasing mean grain size, the sorting ranges between very good and moderate. All samples are characterized by a matrix-supported fabric with grains of quartz, feldspar and rock fragments floating in the matrix. Direct contacts of the grains are rare. Bedding/lamination especially is indicated by grain size variation. Micro-fissures were found in sample Bangudae 1, especially in or along very fine-grained layers.

All samples show a low total porosity. The size of the pores is mainly in the range of micropores and very small capillary pores. The pore surface is relatively high. Comparing the unweathered and weathered parts of Bangudae 2, the weathered part shows a higher total porosity, especially resulting from an increase of small capillary pores due to the dissolution of the carbonate components. The pore surface is higher than in the unweathered part.

With respect to hygric properties, the results are summarized for the unweathered parts of Bangudae 1, 3, 4 and 5 first. As a result of the low porosity, water absorption is low. The ratio between water absorption at atmospheric pressure and maximum water

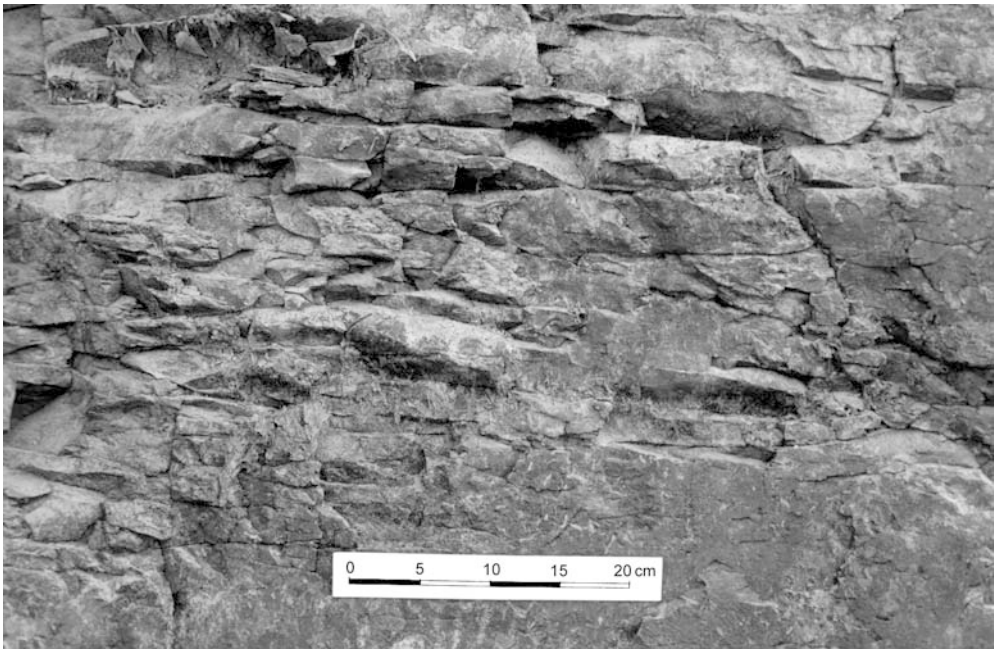

Fig. 8
Weathering form "back weathering due to loss of crumbs (*uW*)"

absorption—expressed by the saturation coefficient S—is high. This high degree of saturation is reached slowly. Considering that the Bangudae Petroglyph is submerged for about 8 months/year, a complete water saturation of the stone material can be assumed during this period. The water desorption of the samples takes place slowly, approximating a constant rest water content remaining in the stone.

With respect to Bangudae 2, it was not possible—due to the size of the sample—to investigate water absorption and desorption separately for unweathered and weathered parts of the sample. Thus, the results must be considered as intermediate between unweathered and weathered condition. They reflect the fact that the water absorption in the weathered part is significantly higher than in the unweathered part, whereas the degree of water saturation is lower in the weathered part. However, in the course of drying a higher percentage of water desorbs in the weathered part than in the unweathered part.

The ultrasonic velocities parallel to bedding are high for sedimentary rocks and reflect the high compactness/hardness of the stone. For the unweathered parts of Bangudae 1 and 2 the ultrasonic velocities perpendicular

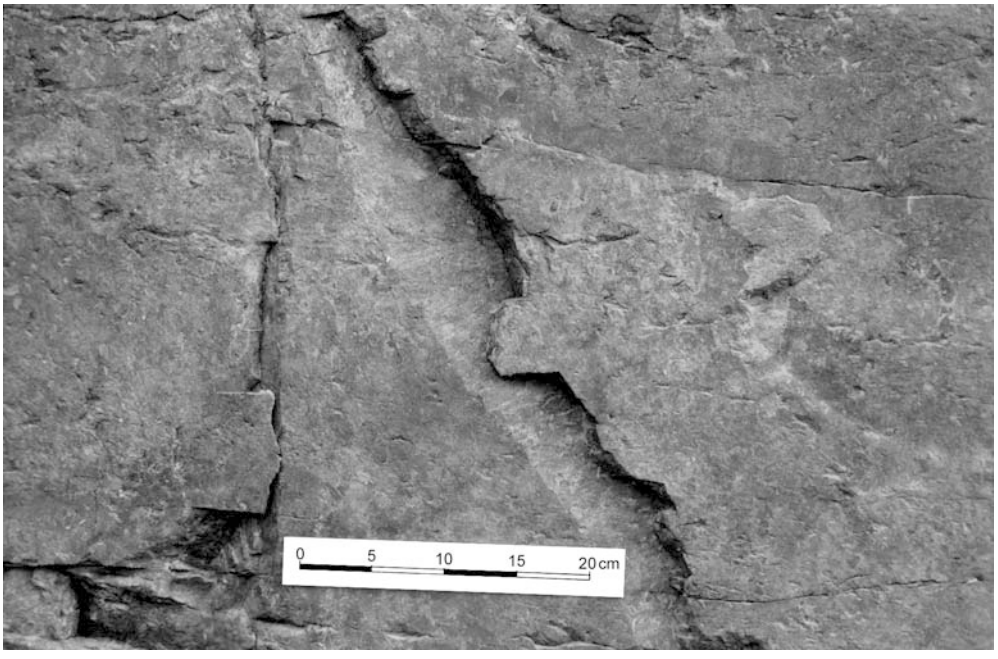

Fig. 9
Weathering form "break out due to natural cause (*nO*)"

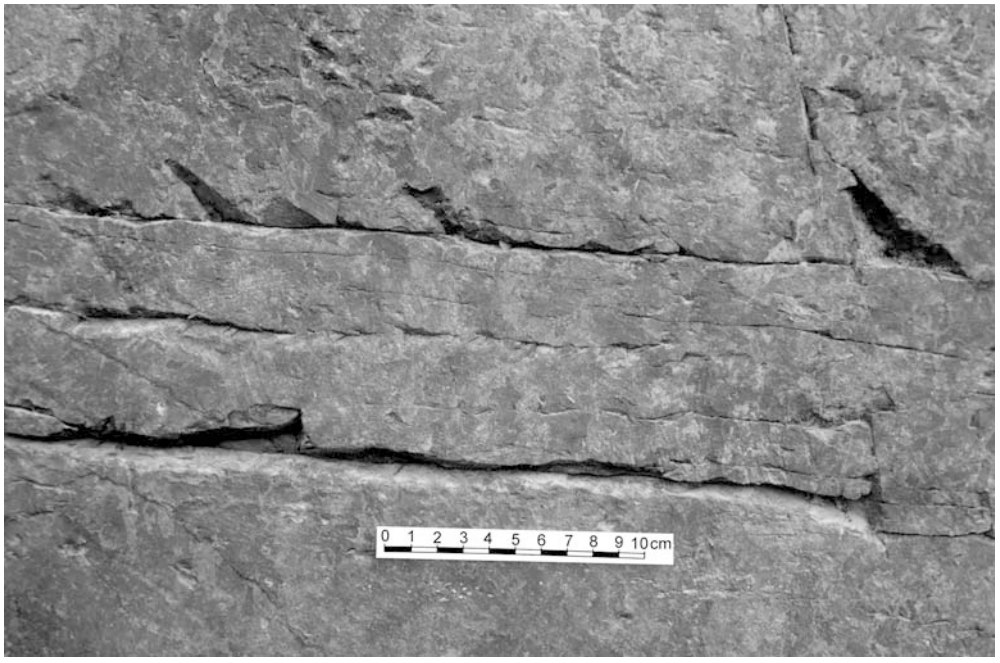

Fig. 10
Weathering form "splitting up (*Xv*)"

to bedding are only slightly lower than those parallel to bedding. This indicates only slight anisotropic characteristics of the stone material. For Bangudae 3–5 lower ultrasonic velocities perpendicular to bedding were determined, which results from fissures. Comparing the unweathered and weathered parts of the sample Bangudae 2, significantly lower ultrasonic velocities were determined for the weathered part indicating a decrease of compactness/hardness.

In the following, the results of monument mapping and measurements are presented. The classification scheme of weathering forms derived for the Bangudae Petroglyph as basis for mapping comprises four levels of differentiation: 4 groups of weathering forms (level I), 14 main weathering forms (level II), 21 individual weathering forms (level III), 21 individual weathering forms with additional differentiation according to intensity (level IV). Some characteristical weathering forms are shown in Figs. 8, 9, 10, 11. The level of highest differentiation—level IV—of the classification scheme was applied for mapping.

In the course of mapping, more than 400 partial areas of the Bangudae Petroglyph were distinguished as a result of

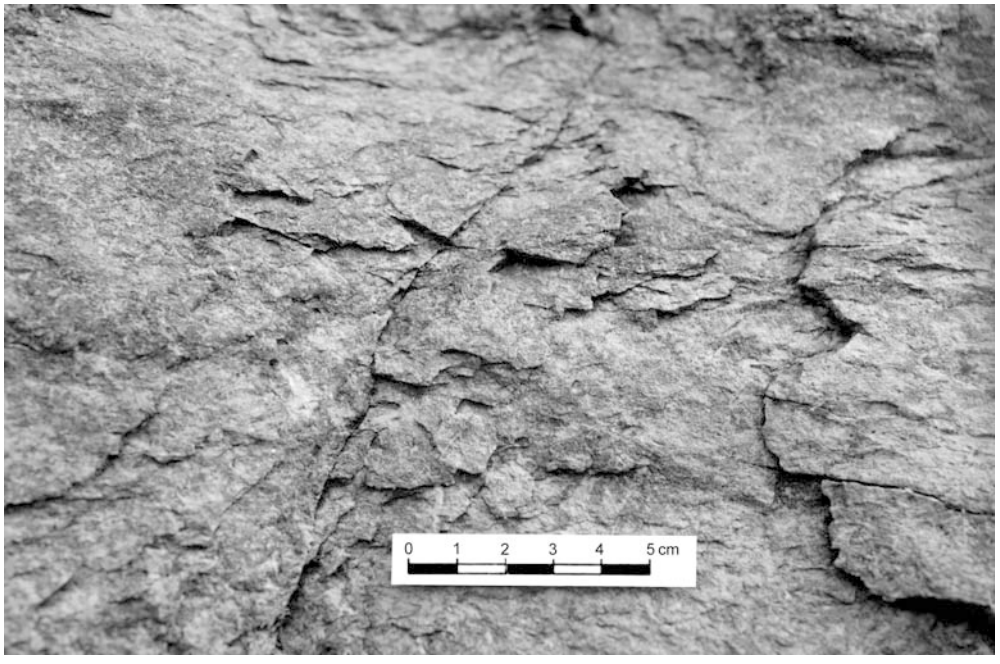

Fig. 11
Weathering form "multiple flakes to crumbling (*mF-Pu*)"

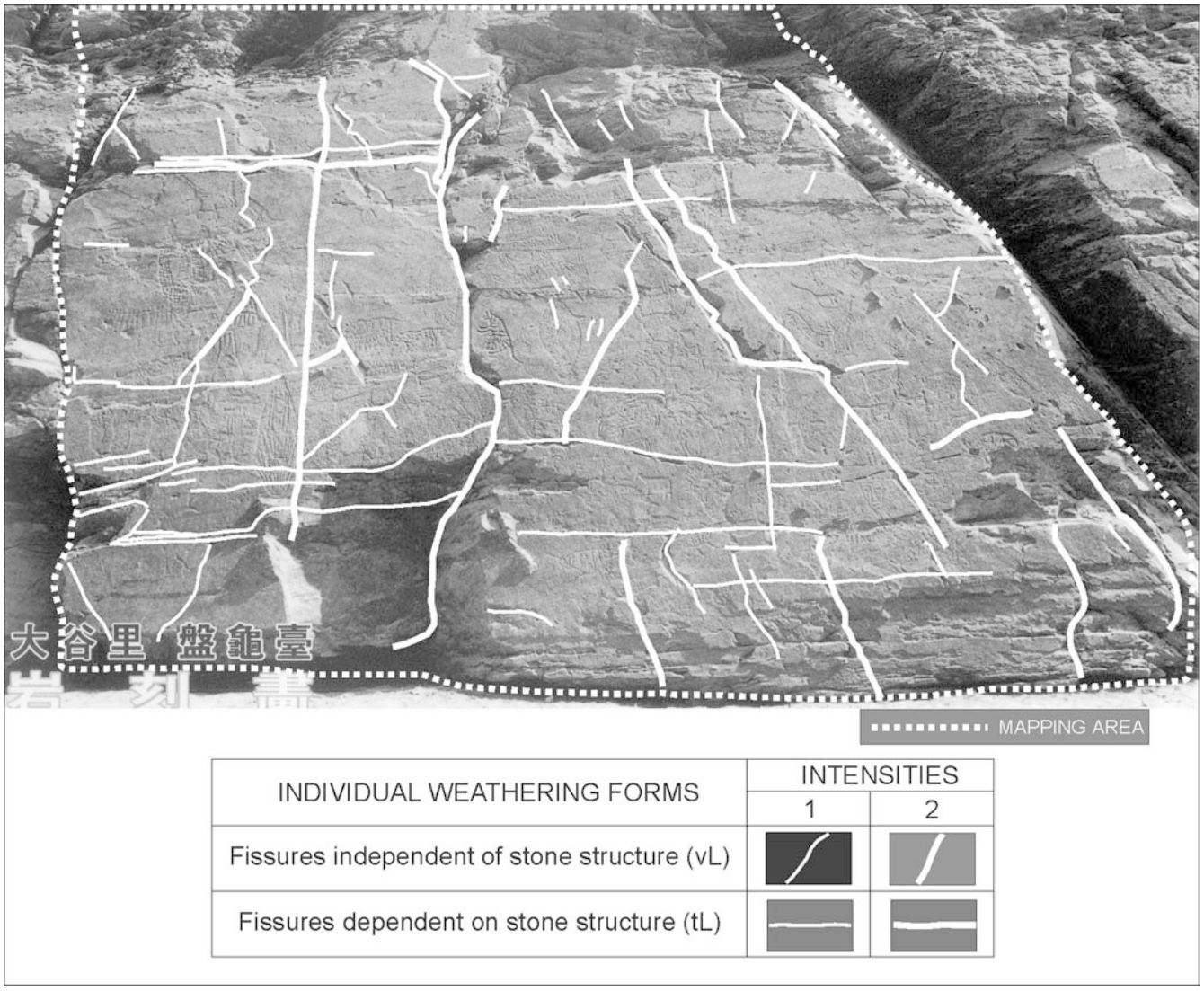

Fig. 12
Mapping of weathering forms. Individual weathering forms: fissures independent of stone structure (*vL*), fissures dependent on stone structure (*tL*)

different types, intensities or combinations of weathering forms. The map of fissures is presented as an example to illustrate the weathering forms (Fig. 12). The quantitative evaluation of the individual weathering forms is shown in Tables 3 and 4.

The most frequent individual weathering forms of group 1 "loss of stone material" are " *back weathering due to loss of crumbs* " and " *break out due to natural cause* ". Back weathering due to loss of crumbs—often with medium to high intensities—is mainly limited to the lower and to the upper part of the investigation area. Break out due to natural cause—with the exception of a huge break out in the lower part—mainly concerns the middle part of the investigation area that contains most of the carvings. It occurs with mainly low to medium intensities, especially along discontinuities. Further weathering forms of group 1 are " *back weathering due to loss of scales* " (mainly in the upper part), "*rounding – notching* " (between middle and upper part), " *weathering out dependent on stone structure*" (middle part) and " *break out due to non-recognizable cause* " (middle part).

Very frequent weathering forms of group 2 "deposits" are " *soiling by particles from the atmosphere or from water* " and " *coloured crust tracing the surface* ". Almost the entire investigation area is affected by these types of deposits. Additionally, " *microbiological colonization* " is irregularly distributed over the stone surface.

Ten individual weathering forms of group 3 "detachment of stone material" were identified. The most frequent weathering form of this group is " *crumbling* ". It particularly affects the lower and the upper part of the investigation area with medium to high intensity. This weathering form is rare in the middle part, where it occurs with mainly low intensity. Less frequent weathering forms of this group are " *single flakes* "(mainly in the middle part), " *single scale* " (irregular distribution), " *splitting up*" (mainly in the middle and upper part), " *single flakes*

Table 3
Quantitative evaluation of the weathering forms of group 1 "loss of stone material" and group 2 "deposits"

Group of weathering forms	Main weathering form	Individual weathering form		Quantitative evaluation of the individual weathering forms considering their intensities									
1 –Loss of stone material	Back weathering (W)	Back weathering due to loss of scales (sW)	Intensity					Depth of back weathering (cm)					
				≤ 0.2		0.2–0.5		0.5–1		1–2		2–5	
			Area-%	*0.41*		*0.73*		*0.60*		*0.31*		–	
		Back weathering due to loss of crumbs (uW)	Intensity					Depth of back weathering (cm)					
				≤ 0.2	0.2 –0.5	0.5–1	1 –2	2 –5	5–10	10–25	25–50	50–75	
			Area-%	–	*0.05*	*3.13*	*3.96*	*6.01*	*7.08*	*3.87*	*1.58*	*2.63*	
	Relief(R)	Rounding / notching (Ro)	Intensity					Depth of relief (cm)					
					≤ 0.2		0.2–0.5		0.5–1		1–2		
			Area-%		*0.42*		*0.18*		*0.22*		*0.16*		
		Weathering out dependent on stone structure (tR)	Intensity					Depth of relief (cm)					
					≤ 0.2			0.2–0.5			0.5 – 1		
			Area-%		*0.51*			*0.08*			–		
	Break out (O)	Break out due to natural cause (nO)	Intensity					Volume of break out (cm^3)					
				≤ 5	5–50	50–500	500–1000	1000–2500	2500–5000	5000–10000	10000–50000	> 50000	
			Area-%	*0.56*	*1.16*	*0.52*	*0.38*	*1.46*	*1.41*	–	–	*4.19*	
		Break out due to non-recognizable cause (oO)	Intensity					Volume of break out (cm^3)					
					≤ 5			5–50			50 – 500		
			Area-%		*0.02*			*0.07*			*0.08*		
2 –Deposits	Soiling(I)	Soiling by particles from the atmosphere or from water (wI)	Intensity					No differentiation					
			Area-%					*96.68*					
	Crust(C)	Coloured crust tracing the stone surface (fkC)	Intensity					No differentiation					
			Area-%					*99.8*					
	Biological coloni-zation (B)	Microbiological colonization (Bi)	Intensity					Degree – covering of the stone surface					
						low				high			
			Area-%			*3.80*				*33.25*			

Table 4
Quantitative evaluation of the weathering forms of group 3 "detachment of stone material"

Group of weathering forms	Main weathering form	Individual weathering form		Quantitative evaluation of the individual weathering forms considering their intensities				
3 – Detachment of stone material	Crumbly disintegration (P)	Crumbling (Pu)	Intensity			Mass of detaching stone material		
					Low	Moderate		High
			Area-%		*7.76*	*10.93*		*13.74*
	Flaking (F)	Single flakes (eF)	Intensity			Mass of detaching stone material		
					Low		Moderate	
			Area-%		*1.68*		–	
	Contour scaling (S)	Single scale (eS)	Intensity			Thickness of the scale (cm)		
				≤ 0.2	0.2–0.5		0.5–1	>1
			Area-%	*0.08*	*0.41*		*0.09*	–
	Detachment of stone layers dependent on stone structure (X)	Splitting up (Xv)	Intensity			Number of detaching stone layers/splits		
					Low		High	
			Area-%		*4.54*		*4.69*	
	Flaking to crumbly disintegration (F-P)	Single flakes to crumbling (eF-Pu)	Intensity			Mass of detaching stone material		
					Low		Moderate	
			Area-%		*4.25*		*0.06*	
		Multiple flakes to crumbling (mF-Pu)	Intensity			Mass of detaching stone material		
					Low		Moderate	
			Area-%		–		*0.29*	
	Crumbly disintegration to contour scaling (P-S)	Crumbling to single scale (Pu-eS)	Intensity			Mass of detaching stone material		
					Low	Moderate		High
			Area-%		*9.17*	*1.79*		–
		Crumbling to multiple scales(Pu-mS)	Intensity			Mass of detaching stone material		
					Low	Moderate		High
			Area-%		–	*2.39*		*0.71*
	Flaking to contour scaling (F-S)	Single flakes to single scale (eF-eS)	Intensity			Mass of detaching stone material		
					Low		Moderate	
			Area-%		*1.10*		–	
		Multiple flakes to multiple scales (mF-mS)	Intensity			Mass of detaching stone material		
					Low	Moderate		High
			Area-%		*0.69*	*0.26*		*0.29*

to crumbling " (mainly in the middle and upper part), "*multiple flakes to crumbling*", "*crumbling to single scale*" (lower and upper part), "*crumbling to multiple scales*" (lower and upper part), "*single flakes to single scale*" (lower and upper part) and "*multiple flakes to multiple scales*" (upper part). It can be stated that detachment of stone material is concentrated in the lower and the upper parts of the investigation area, whereas frequency and intensity are lower in the middle part.

Two weathering forms of group 4 "fissures" were distinguished: "*fissures independent of stone structure*" and "*fissures dependent on stone structure*". These weathering forms are characteristic of the whole investigation area. In contrast to fissures dependent on stone structure, the intensity of the fissures independent of stone structure is high.

With respect to combinations of weathering forms, the quantitative evaluation revealed four different cases. The numbering of the cases from 1 to 4 is considered to correlate with the chronological order in which they occur on the monument.

Case 1 The stone surface is only affected by weathering forms of group 2 "deposits", mostly a combination of soiling, crust formation and biological colonization. Case 1 concerns 45.0% of the investigation area.

Case 2 Weathering forms of group 2 "deposits" and group 3 "detachment of stone material" occur in combination. Case 2 concerns 12.9% of the investigation area.

Case 3 The stone surface is affected by combinations of weathering forms of group 1 "loss of stone material"

Table 5
Correlation scheme "weathering forms–damage categories" for the weathering forms of group 1 "loss of stone material" and group 2 "deposits"

Group of weathering forms	Main weathering form	Individual weathering form		Relating of the individual weathering forms to damage categories considering the intensities of the weathering forms								
1 –Loss of stone material	Back weathering (W)	Back weathering due to loss of scales (sW)	Intensity	Depth of back weathering (cm)								
				≤ 0.2	0.2–0.5	0.5–1	1–2	2–5				
			Damage category	*4*	*5*	*5*	*5*	*5*				
		Back weathering due to loss of crumbs (uW)	Intensity	Depth of back weathering (cm)								
				≤ 0.2	0.2–0.5	0.5–1	1–2	2–5	5–10	10–25	25–50	50–75
			Damage category	*4*	*5*	*5*	*5*	*5*	*5*	*5*	*5*	*5*
	Relief (R)	Rounding/ notching (Ro)	Intensity	Depth of relief (cm)								
				≤ 0.2		0.2–0.5		0.5–1		1–2		
			Damage category	*4*		*5*		*5*		*5*		
		Weathering out dependent on stone structure (tR)	Intensity	Depth of relief (cm)								
				≤ 0.2		0.2–0.5				0.5–1		
			Damage category	*4*		*5*				*5*		
	Break out (O)	Break out due to natural cause (nO)	Intensity	Volume of break out (cm^3)								
				≤ 5	5–50	50–500	500–1000	1000–2500	2500–5000	5000–10000	10000–50000	>50000
			Damage category	*2*	*3*	*4*	*5*	*5*	*5*	*5*	*5*	*5*
		Break out due to non-recognizable cause (oO)	Intensity	Volume of break out (cm^3)								
					≤ 5			5–50			50–500	
			Damage category		*2*			*3*			*4*	
2–Deposits	Soiling (I)	Soiling by particles from the atmosphere or from water (wI)	Intensity	No differentiation								
			Damage category	*1*								
	Crust (C)	Coloured crust tracing the stone surface (fkC)	Intensity	No differentiation								
			Damage category	*1*								
	Biological coloni-zation (B)	Microbiological colonization (Bi)	Intensity	Degree–covering of the stone surface								
						Low				High		
			Damage category			*1*				*2*		

Table 6
Correlation scheme "weathering forms–damage categories" for the weathering forms of group 3 "detachment of stone material"

Group of weathering forms	Main weathering form	Individual weathering form	Relating of the individual weathering forms to damage categories considering the intensities of the weathering forms				
3 – Detachment of stone material	Crumbly disintegration (P)	Crumbling (Pu)	Intensity		Mass of detaching stone material		
				Low	Moderate	High	
			Damage category	*3*	*4*	*5*	
	Flaking (F)	Single flakes (eF)	Intensity		Mass of detaching stone material		
				low	moderate		
			Damage category	*2*	*3*		
	Contour scaling (S)	Single scale (eS)	Intensity		Thickness of the scale (cm)		
				≤ 0.2	0.2–0.5	0.5–1	>1
			Damage category	*3*	*4*	*5*	*5*
	Detachment of stone layers dependent on stone structure (X)	Splitting up (Xv)	Intensity		Number of detaching stone layers/splits		
				Low	High		
			Damage category	*3*	*4*		
	Flaking to crumbly disintegration (F-P)	Single flakes to crumbling (eF-Pu)	Intensity		Mass of detaching stone material		
				Low	Moderate		
			Damage category	*3*	*4*		
		Multiple flakes to crumbling (mF-Pu)	Intensity		Mass of detaching stone material		
				Low	Moderate		
			Damage category	*3*	*4*		
	Crumbly disintegration to contour scaling (P-S)	Crumbling to single scale (Pu-eS)	Intensity		Mass of detaching stone material		
				Low	Moderate	High	
			Damage category	*3*	*4*	*5*	
		Crumbling to multiple scales(Pu-mS)	Intensity		Mass of detaching stone material		
				Low	Moderate	High	
			Damage category	*3*	*4*	*5*	
	Flaking to contour scaling (F-S)	Single flakes to single scale (eF-eS)	Intensity		Mass of detaching stone material		
				Low	Moderate		
			Damage category	*2*	*3*		
		Multiple flakes to multiple scales (mF-mS)	Intensity		Mass of detaching stone material		
				Low	Moderate	High	
			Damage category	*2*	*3*	*4*	

and group 2 "deposits". Case 3 concerns 2.8% of the investigation area.
Case 4 The stone surface is affected by combinations of weathering forms of group 1 "loss of stone material", group 2 "deposits" and group 3 "detachment of stone material". Case 4 concerns 39.3% of the investigation area.

The cases 1–3 mainly affect the middle part of the investigation area that contains most of the carvings, whereas case 4 is mainly limited to the lower and upper parts of the investigation area.
Based on the classification and mapping of weathering forms and their intensities, damage categories and a damage index were established for the quantification and rating of weathering damage. Six damage categories were defined: 0 – no visible damage, 1 – very slight damage, 2 – slight damage, 3 – moderate damage, 4 – severe damage, 5 – very severe damage.

A correlation scheme was developed for the Bangudae Petroglyph, in which all observed weathering forms—considering their type and intensity—are related to damage categories. The high historical value of the Bangudae Petroglyph was taken into account. Additionally, results obtained from the measurements on site were considered. The correlation scheme of weathering forms to damage categories is presented in Tables 5 and 6. Based on this correlation scheme, damage categories were determined separately for group 1 of weathering forms "loss of stone material", group 2 of weathering forms "deposits" and group 3 of weathering forms "detachment of stone material". In the next step of the evaluation, damage categories were determined considering all weathering forms of groups 1–3 in combination. The damage categories are illustrated in maps (Figs. 13, 14, 15, 16) and are evaluated quantitatively including calculation of the damage index (Table 7).

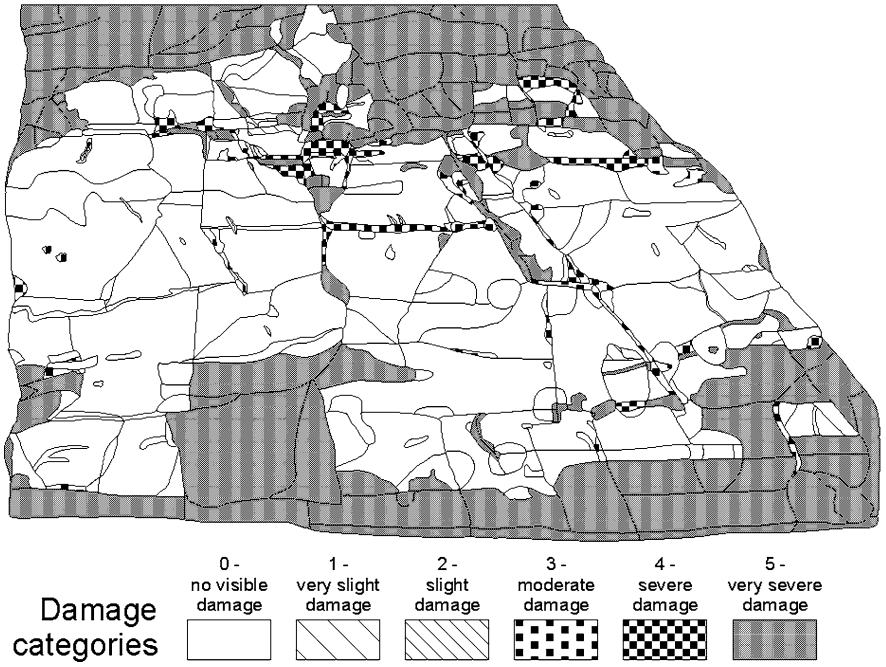

Fig. 13
Damage categories for all weathering forms of group 1 "loss of stone material"

With respect to damage categories for all weathering forms of group 1 "loss of stone material", no damage (damage category 0) and very severe damage (damage category 5) are prevailing on the investigation area. Very severe damage especially concerns the lower and upper parts of the investigation area. Slight, moderate and severe damage (damage categories 2–4) are limited to the middle part of the petroglyph.
Considering the damage categories for all weathering forms of group 2 "deposits", very slight damage (damage category 1) and slight damage (damage category 2) prevail. With respect to damage categories for all weathering forms of group 3 "detachment of stone material", no damage (damage category 0) is prevalent, especially on the middle part of the investigation area with most of the carvings. Slight damage (damage category 2) and moderate damage (damage category 3) mainly concern the transitional areas between middle part and lower respectively upper part of the investigation area. Severe damage (damage category 4) and very severe damage (damage category 5) are found mainly in the lower and the upper part of the investigation area.

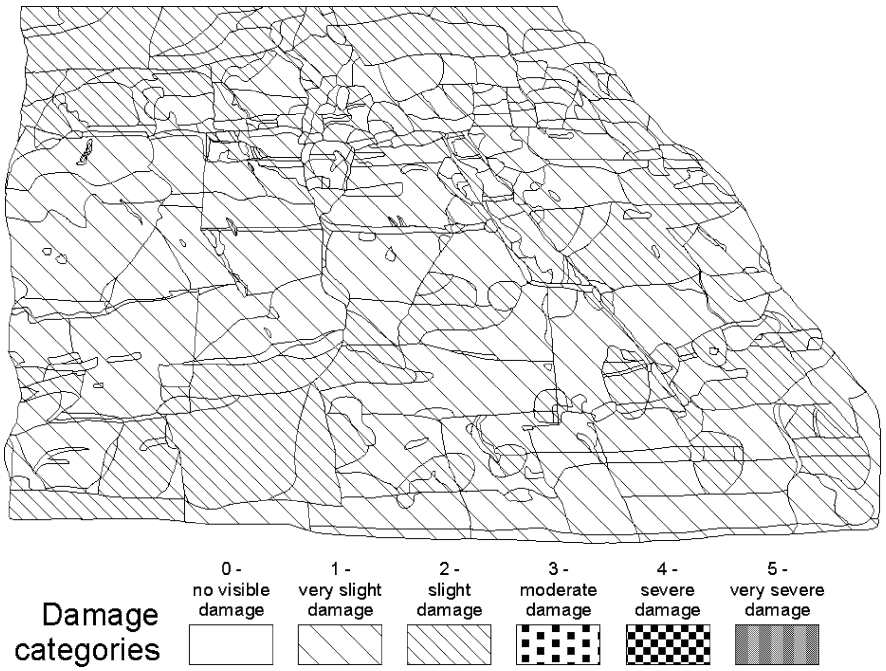

Fig. 14
Damage categories for all weathering forms of group 2 "deposits"

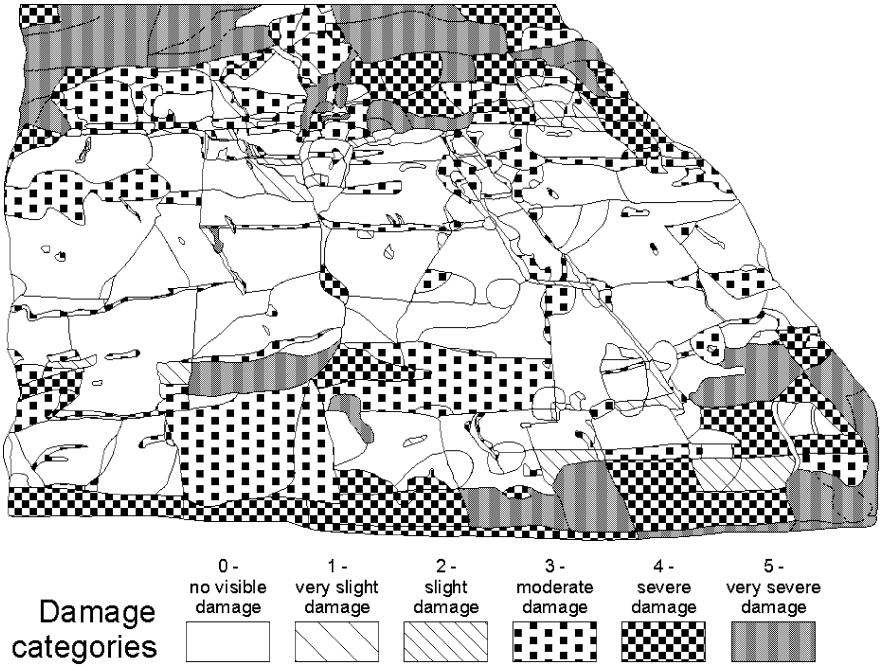

Fig. 15
Damage categories for all weathering forms of group 3 "detachment of stone material"

The damage categories for all weathering forms of group 1 "loss of stone material", group 2 "deposits" and group 3 "detachment of stone material" in combination show that very slight damage (damage category 1) and very severe damage (damage category 5) prevail. Very slight damage is mainly limited to the middle part of the investigation area and very severe damage (damage category 5) is mainly found in the lower and upper parts of the investigation area. Slight damage (damage category 2), moderate damage (damage category 3) and severe damage (damage category 4) are very characteristic of the transition areas between middle and lower parts and between middle and upper parts of the investigation area respectively.

Considering that the damage index can range between 0 and 5.0 per definition, the damage indices regarding loss of stone material (2.02) and detachment of stone material (1.95) are low to moderate and the damage index for deposits (1.34) is low. The damage index for all weathering forms of the groups 1–3 in combination is rather high (2.96).

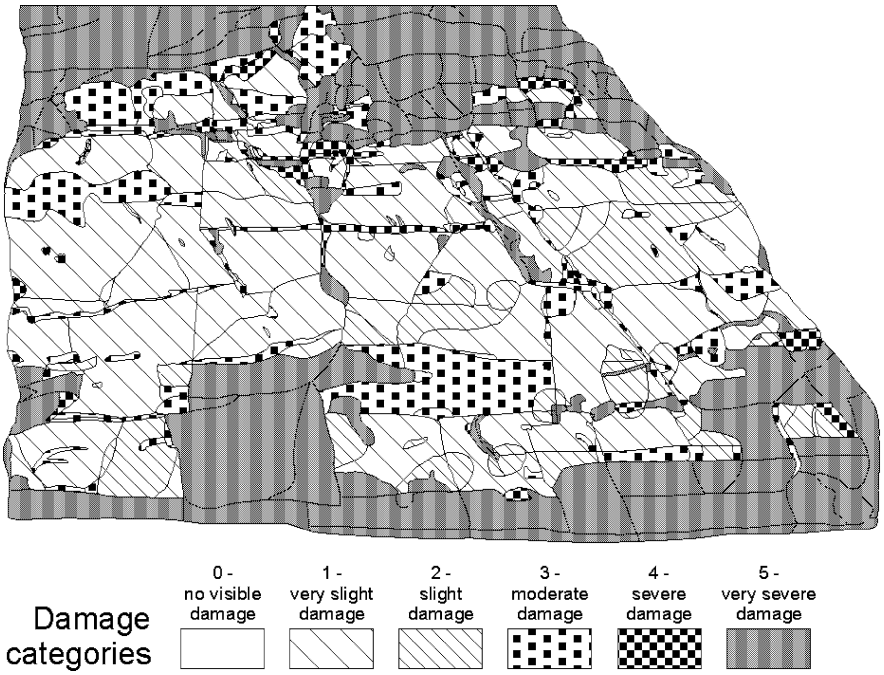

Fig. 16
Damage categories considering all weathering forms of group 1 "loss of stone material", group 2 "deposits" and group 3 "detachment of stone material" in combination

Table 7
Quantitative evaluation of damage categories and calculation of the damage index

Groups of weathering forms considered	Damage category 0 – no visible damage (area-%)	Damage category 1 – very slight damage (area-%)	Damage category 2 – slight damage (area-%)	Damage category 3 – moderate damage (area-%)	Damage category 4 – severe damage (area-%)	Damage category 5 – very severe damage (area-%)	*Damage index*
Group 1 – loss of stone material	58.54	–	0.35	1.18	1.89	38.04	*2.02*
Group 2 – deposits	0.08	65.75	34.17	–	–	–	*1.34*
Group 3 – detachment of stone material	48.37	–	2.92	20.07	14.06	14.58	*1.95*
Group 1, group 2 and group 3 in combination	0.08	37.02	9.79	11.97	2.60	38.54	*2.96*

Damage index DI

$$DI = \frac{(A \cdot 0) + (B \cdot 1) + (C \cdot 2) + (D \cdot 3) + (E \cdot 4) + (F \cdot 5)}{100} = \frac{B + (C \cdot 2) + (D \cdot 3) + (E \cdot 4) + (F \cdot 5)}{100} \qquad 0 \le \mathrm{DI} \le 5$$

A = Area (%) – damage category 0
B = Area (%) – damage category 1
C = Area (%) – damage category 2
D = Area (%) – damage category 3
E = Area (%) – damage category 4
F = Area (%) – damage category 5

$$\sum_{A}^{F} = 100$$

Ultrasonic velocities were used to quantify the weathering state of the rocks, especially with respect to disintegration/detachment of stone material and discontinuities/fissures. They are mapped as isolines in Fig. 17. Their distribution is classified in Fig. 18. The highest ultrasonic velocities of about 4,400 m/s correspond to the ultrasonic velocities determined for the unweathered parts of the analyzed samples. Ultrasonic velocities decrease as the

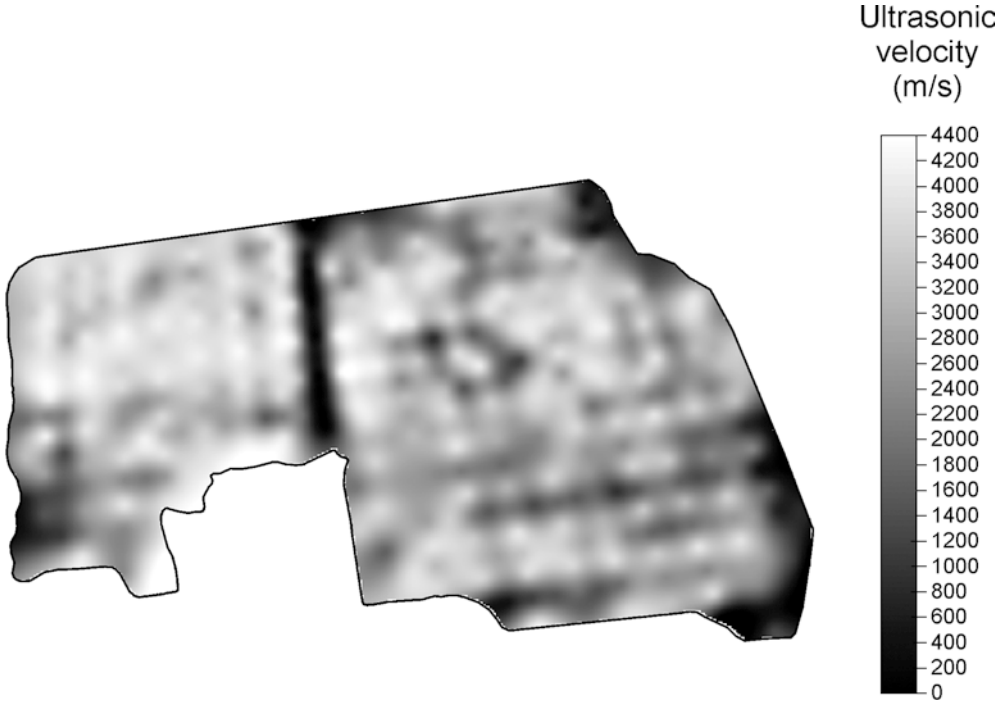

Fig. 17
Ultrasonic measurements. Map of ultrasonic velocities

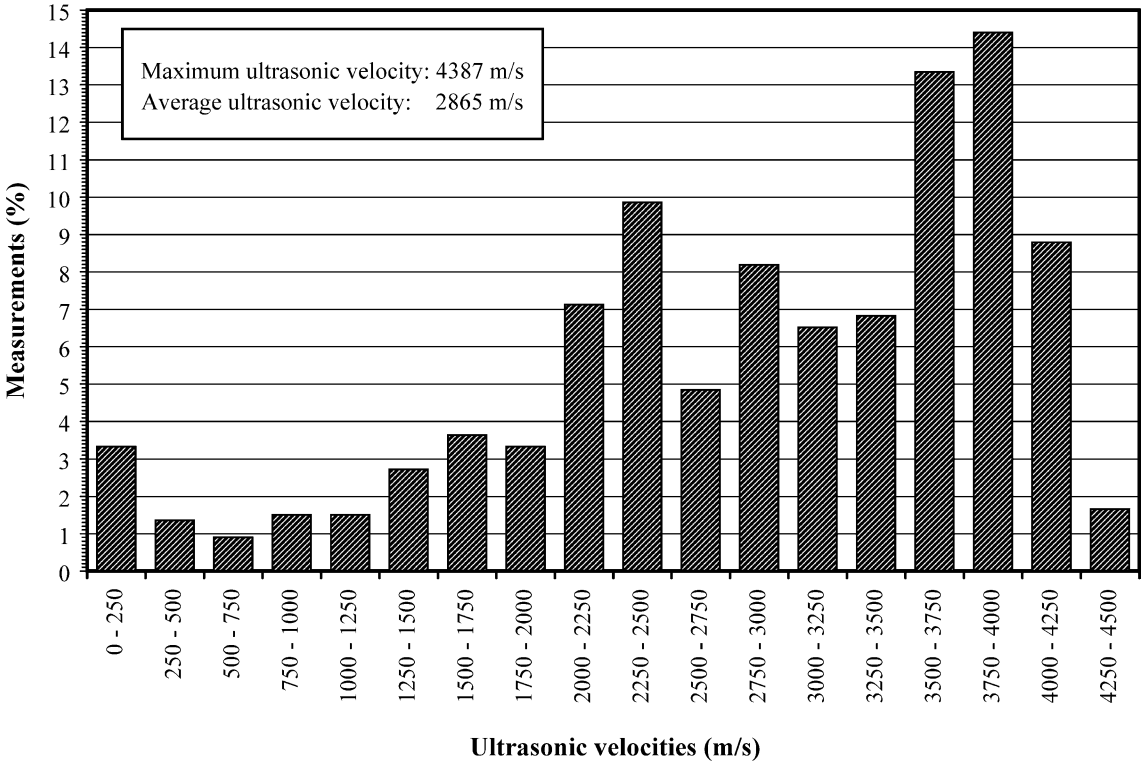

Fig. 18
Classification of the ultrasonic velocities

intensity of disintegration/detachment of stone material and the dimension of discontinuities (depth, width) increase. In Fig. 17 the transition from unweathered rocks to increasing deterioration of rocks correlates with the transition from light grey to black colour. The colour pattern clearly reflects and quantifies a significant network of individual or intersecting discontinuities and the map is an important supplement to the fissure map (Fig. 12). High to very high ultrasonic velocities (3,500–4,400 m/s, 40% of the measurements) are mainly limited to the upper part of the investigation area —especially to the upper left part, whereas medium, low and very low ultrasonic velocities in the lower part and in the upper right part are correlated with relatively intense stone detachment.

The rebound hardness measuring procedure is illustrated in Fig. 19 and the distribution of the rebound hardnesses is classified in Fig. 20. The registered rebound hardnesses range between 19 and 56. The rebound hardness for non-carved areas without any detachment of stone material ranges between 45 and 56 (average: 49). It is striking that the rebound hardness for carved areas without any visible stone deterioration is considerably lower. It ranges between 34 and 46 (average: 41). This indicates a weakening of the grain-bond due to the carving procedure. With respect to detachment of stone material, the lowest rebound hardnesses were stated for stone surfaces affected by intense crumbly disintegration. Considering the rather high average rebound hardnesses related to other types of detachment of stone material, it can be deduced that the detaching stone pieces are still well-connected to the stone beneath. Therefore, a rapid loss of stone material in the near future is not very probable.

Results obtained from the evaluation of weathering forms and from the in situ measurements (ultrasonic measurements, rebound hardness measurements) were combined for the characterization and quantification of damage zones.

Based on monument mapping, a vertical profile of the damage index was determined for the investigation area. Additionally, ultrasonic velocities and rebound hardnesses were evaluated with respect to a vertical profile (Fig. 21).

Fig. 19
Rebound hardness measurements with a Schmidt hammer

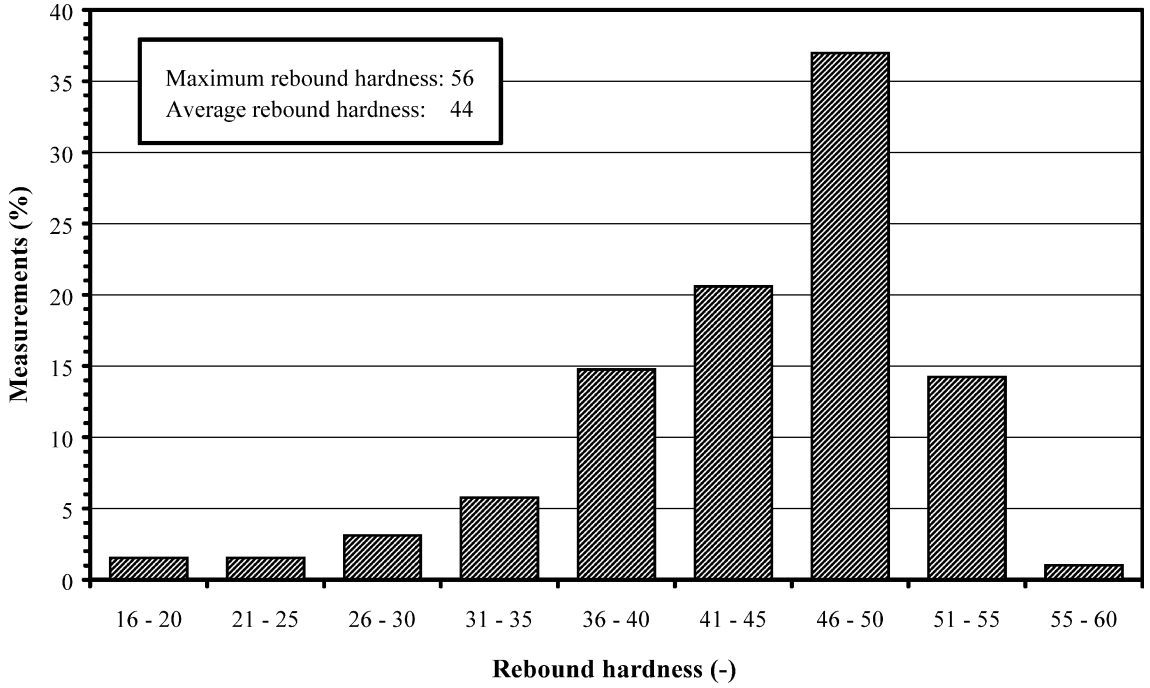

Fig. 20
Classification of the rebound hardnesses

The profile of average ultrasonic velocities correlates with the profile of average rebound hardnesses, whereas these profiles are inversely proportional to the profile of damage index.
Combining the results, five zones of damage were distinguished (Fig. 22, Table 8). Zones 2–4 relate to the part of the investigation area, where most of the carvings are found.

Zone 1 (height: 0–60 cm)
This lowermost zone shows the most severe damage. Compared to the zones 2–4 following upwards, it is characterized by the highest damage index and the lowest average ultrasonic velocity and rebound hardness. Considering that the damage index can range between 0 and 5 per definition, the damage index of 4.9 determined for this zone is alarming. High frequency and intensity referring to loss of stone material, detachment of stone material and fissures are characteristic for this zone. Zone 1 undercuts the parts with most of the carvings following upwards. Break out of stone material on these parts, especially along the many steeply inclined discontinuities, can result from this undercutting.

Zone 2 (height: 60–170 cm)
This zone represents a transitional zone between the severely damaged lowermost zone 1 and the rather well-preserved zone 3. The damage index of 2.8 is rather high, the average ultrasonic velocity is low to moderate and the average rebound hardness is moderate.
Number and dimension of fissures are comparable to zone 1, whereas frequency and intensity referring to loss and detachment of stone material is lower. However, a huge break out of stone material affects this zone.

Zone 3 (height: 170–290 cm)
This zone represents a well-preserved part of the investigation area. The damage index of 1.6 can be considered as low. Loss of stone material and detachment of stone material are rare, their intensity is mainly low. Therefore, the average rebound hardness is high. However, the moderate average ultrasonic velocity reflects the considerable number and dimension of fissures in this zone.

Zone 4 (height: 290–360 cm)
This zone represents a transitional zone between the well-preserved zone 3 and the severely damaged uppermost zone 5. The damage index of 2.8 is rather high, the average ultrasonic velocity and the average rebound hardness are moderate. Frequency and intensity with respect to loss of stone material and detachment of stone material can be considered as moderate. A considerable number and dimension of fissures can be stated.

Zone 5 (height: 360–510 cm)
This uppermost zone shows severe damage. The high damage index of 4.5 is alarming. Loss of stone material and detachment of stone material – with mainly high intensity—and fissures are characteristic for this zone. Although no measurements were made at this part, ultrasonic velocity and rebound hardness are expected to be low.
Profile measurements were made at 40 carvings distributed all over the investigation area (Fig. 23). Examples of carvings with indications of the measuring section and the profiles are illustrated in Fig. 24. The white areas in the

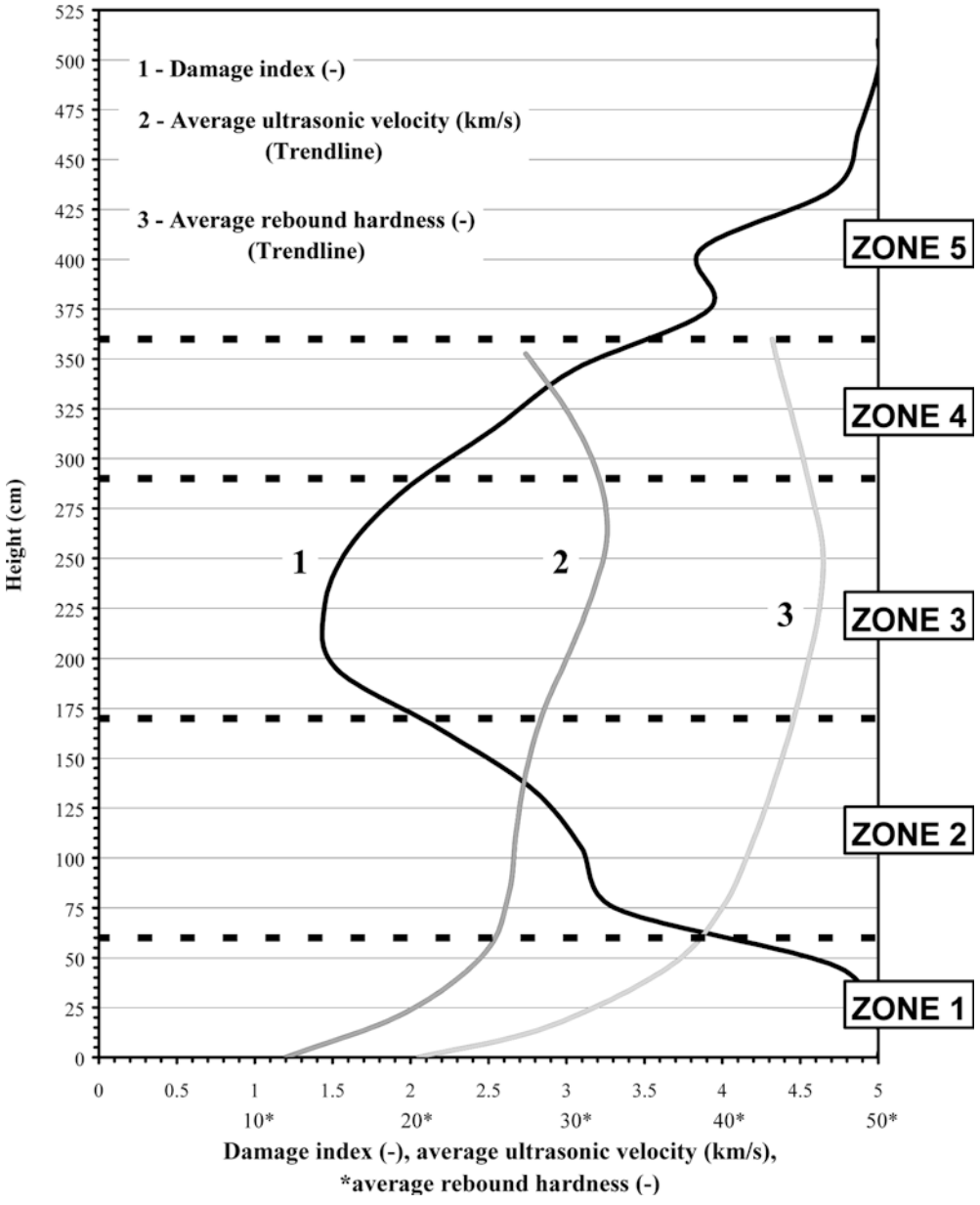

Fig. 21
Zonation of damage – vertical profile

profiles represent the stone material removed by carving, the grey areas the remaining stone material. Fig. 25 shows the evaluation of all profiles with respect to the maximum depth and the average depth. All profiles show a maximum depth of less than 4 mm. The maximum depth of most of the profiles is between 2 and 3 mm and average depth is between 1 and 2 mm. This quantitative evaluation of the profiles was used for a risk prognosis (Fig. 26). For example, if the stone surface were to recede 2 mm, at least 20% of the carvings would be lost. If it were to recede 3 mm, almost 80% of the carvings would be lost. This prognosis is alarming, considering the recent stone detachment—described by weathering forms such as granular disintegration, flaking, contour scaling and crumbling—and structural/textural weakening of the rocks indicated by the lower ultrasonic velocities and rebound hardnesses.

Discussion

The Bangudae Petroglyph in the area of Ulsan Metropolitan City has an outstanding archaeological and cultural value. It is of vital importance for the history and the identity of the country. The petroglyph was apparently exposed to rather favourable environmental conditions over a very long period. Since the construction of the Sayeon dam—finished in 1965—the petroglyph is periodically submerged by the Sayeon reservoir, which is considered to endanger this important cultural heritage. Additionally, the dense network of fissures bears the risk of structural instability or even the break out of compact stone fragments. This has already happened frequently. The protection of the Bangudae Petroglyph has become an important concern.

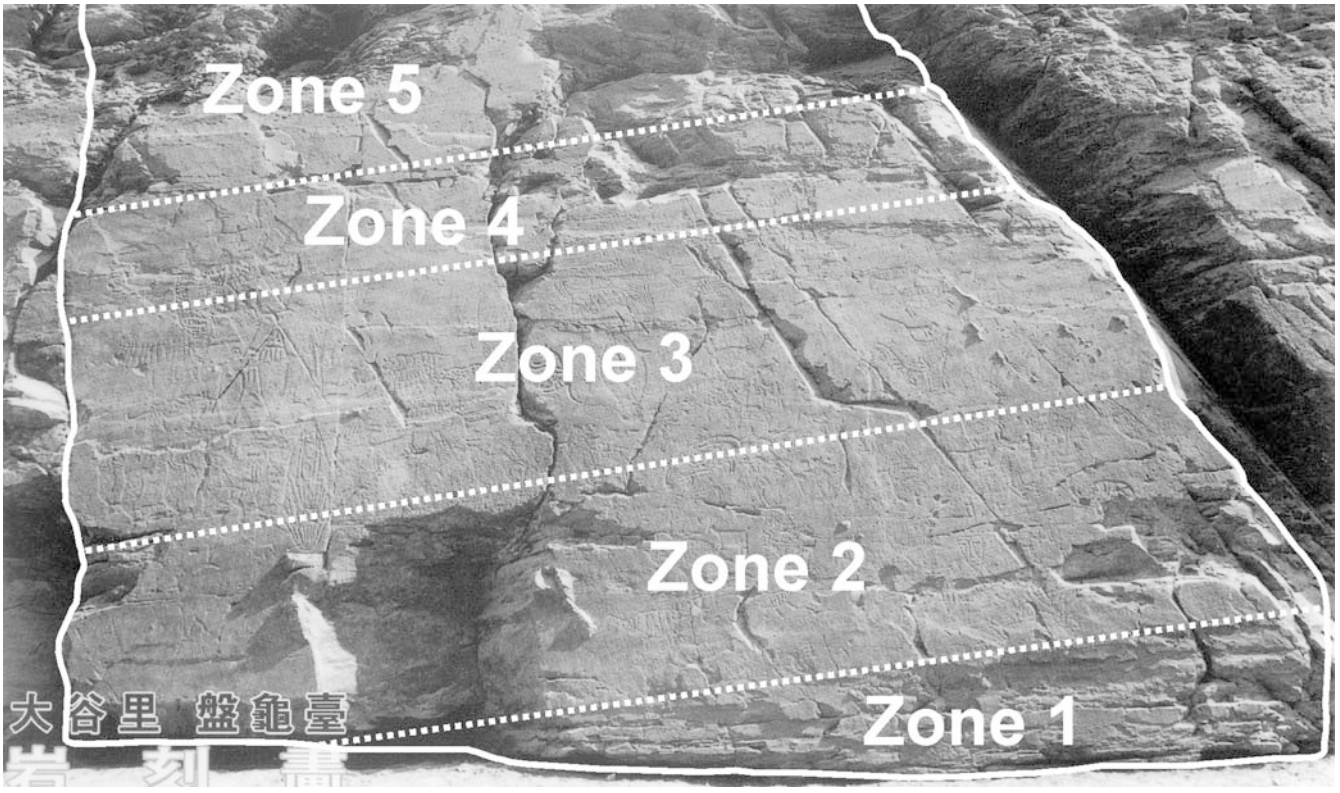

Fig. 22
Zonation of damage

On behalf of Ulsan Metropolitan city and in close cooperation with the Department of Geological Sciences/Seoul National University–Republic of Korea, the working group "Natural stones and weathering" of the Geological Institute/RWTH Aachen University–Germany has carried out studies on the Bangudae Petroglyph focussed on a scientific diagnosis of stone damage. The studies have combined in situ investigation—monument mapping and various systematic measurements—and laboratory analysis of representative stone samples.

Weathering forms were used for the assessment of the weathering state according to phenomenological criteria. Based on a detailed classification scheme of weathering forms developed for the Bangudae Petroglyph, the investigation area was mapped with respect to type, intensity and combination of weathering forms. A remarkable range of weathering forms and their intensities and combinations was found concerning loss of stone material, deposits on stone surface, current detachment of stone material and discontinuities (fissures). More than 400 partial areas were distinguished as a result of 170 different situations referring to types, intensities and combinations of weathering forms. This reveals a rather complex weathering state of the petroglyph that has to be faced.

The central part of the petroglyph containing most of the carvings is significantly less affected by loss of stone material and current detachment of stone material than the marginal lower and upper parts of the investigation area. However, it is subject to fissuring and a considerable number of fissures with varying dimensions were found in the lower and the upper parts of this section. Crumbly disintegration—often of high intensity—is very characteristic in the lower and the upper parts of the investigation area where it has resulted in considerable back weathering.

Table 8
Zonation of damage

Zone	Height (cm)	Average damage index (–)	Average ultrasonic velocity (m/s)	Average rebound hardness (–)
5	360 – 510	4.5	No measurements, expected to be low	No measurements, expected to be low
4	290 – 360	2.8	2960	44
3	170 – 290	1.6	3140	46
2	60 – 170	2.8	2730	43
1	0 – 60	4.9	1830	33

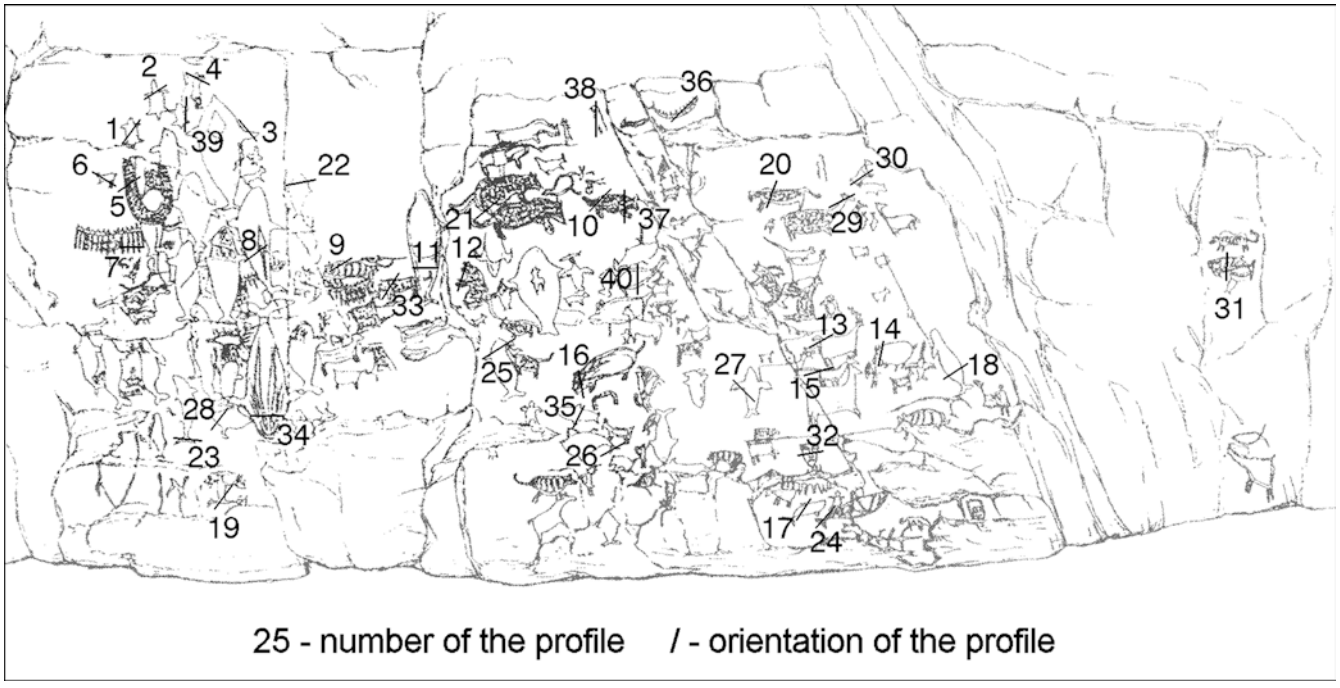

Fig. 23
Profile measurements. Location and orientation of the profiles

Ultrasonic measurements and rebound hardness measurements were carried out for stone characterization and for quantification of stone deterioration. High ultrasonic velocities and rebound hardnesses indicate high compactness/hardness of the stone material when not affected by disintegration. Low ultrasonic velocities in all parts of the investigation area especially reflect the intense network of fissures. Very low ultrasonic velocities in the lower part additionally reveal intense detachment of stone material. This is also indicated by low rebound hardnesses.
In case of no visible stone deterioration, the rebound hardnesses determined for areas with carvings are considerably lower than those determined for the non-carved areas due to mechanical impact of the carving procedure. This finding displays the carved parts as more sensitive to future deterioration than non-carved parts.
Results obtained from monument mapping, ultrasonic measurements and rebound hardness were combined for the evaluation of damage zonation. The investigation area was subdivided into five damage zones. The lowermost and the uppermost parts (zones 1 and 5) represent the zones of very severe damage. High frequency and intensity concerning loss of stone material, current detachment of stone material and fissures are characteristic for these zones. Zones 2–4 concern the part of the investigation area that contains most of the carvings. Loss of stone material and current detachment of stone material are rare in zone 3. Very slight to slight damage is prevailing, rarely moderate, severe or very severe damage are stated. However, this zone is affected considerably by fissures. Zones 2 and 4 represent transitional zones between zones 1 and 3, respectively 3 and 5. Damage can be considered as moderate to high. Fissures are characteristic for these zones, too. The lowermost zone 1 undercuts those parts where are the majority of carvings. Owing to the disintegration and detachment of stone material in zone 1, the undercutting will increase in the future. Therefore, the undercutting bears the considerable risk that parts with carvings will break off.
The profile measurements at carvings have shown that the maximum depth of the carvings is between 2 and 3 mm. Macroscopic detachment of stone material at the carvings is rather rare. The actual low relief of many carvings is considered as a result of erosion provoked by non-visible detachment of finest particles. The low relief of the carvings means that the high historical and cultural importance of the petroglyph is limited to a stone surface zone of only few millimetres. So, even slightest erosion will result in the disappearance of carvings. This prognosis is alarming.
According to the results obtained from the laboratory analysis of stone samples, the Bangudae Petroglyph was carved from compact, silty, carbonatic mudstones, which—in unweathered state—are characterized by low porosity (mainly micropores and small capillary pores), relatively high pore surface and low water absorption capacity. According to the water desorption tests, even in the dry season the stone retains a considerable moisture content. The most striking characteristic of weathered parts of the mudrocks is the dissolution of carbonate resulting in an increase of porosity especially by small capillary pores, an increase of water absorption capacity and a decrease of compactness/hardness. Thus, submerging by the Sayeon reservoir water means a considerable risk to the petroglyph with respect to chemical decomposition. Additionally, moistening of stone—moistening due to submerging and natural

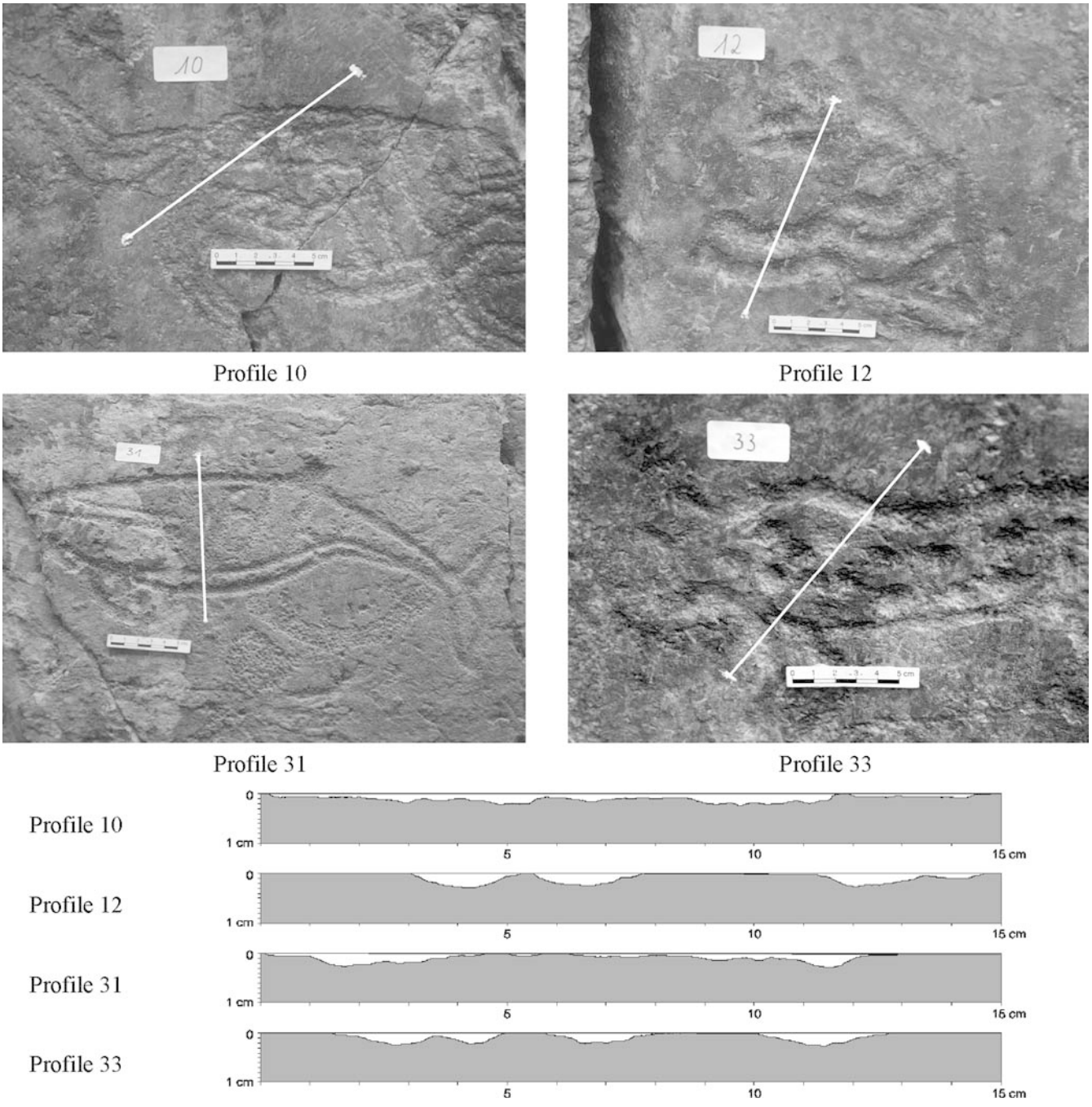

Fig. 24
Profile measurements—examples

moistening in winter—is considered as a risk regarding physical disintegration.

Preservation measures—especially preventive measures—are advisable. The presented results of damage diagnosis will be combined with information from other disciplines such as rock mechanics, hydrology/hydrogeology, climatology and engineering sciences. Then an appropriate preservation strategy will be decided. At present, the continuous monitoring of the Bangudae Petroglyph is recommended in order to recognize any damage progression and to eventually initiate immediate intervention. Structural reinforcement, protection against submerging (e.g. by a protective dam), stone conservation—based on careful test application—and appropriate site management are advised steps for the preservation of the Bangudae petroglyph.

Acknowledgements The authors would like to express their gratitude to the authorities of Ulsan Metropolitan City for the financial support of the studies on the Bangudae Petroglyph. The authors would like to thank Prof. Dr. Soo Jin Kim and his team from the Department of Geological Sciences, Seoul National University, for the cooperation, discussions and advice and for all logistical support of the works.

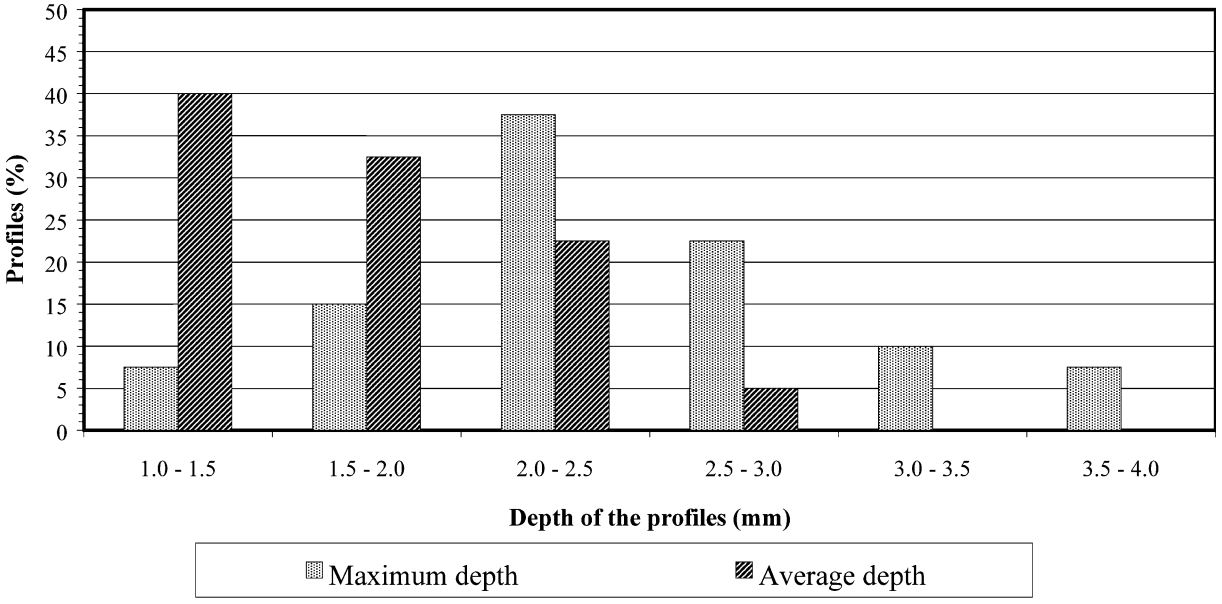

Fig. 25
Profile measurements. Classification of maximum and average depths

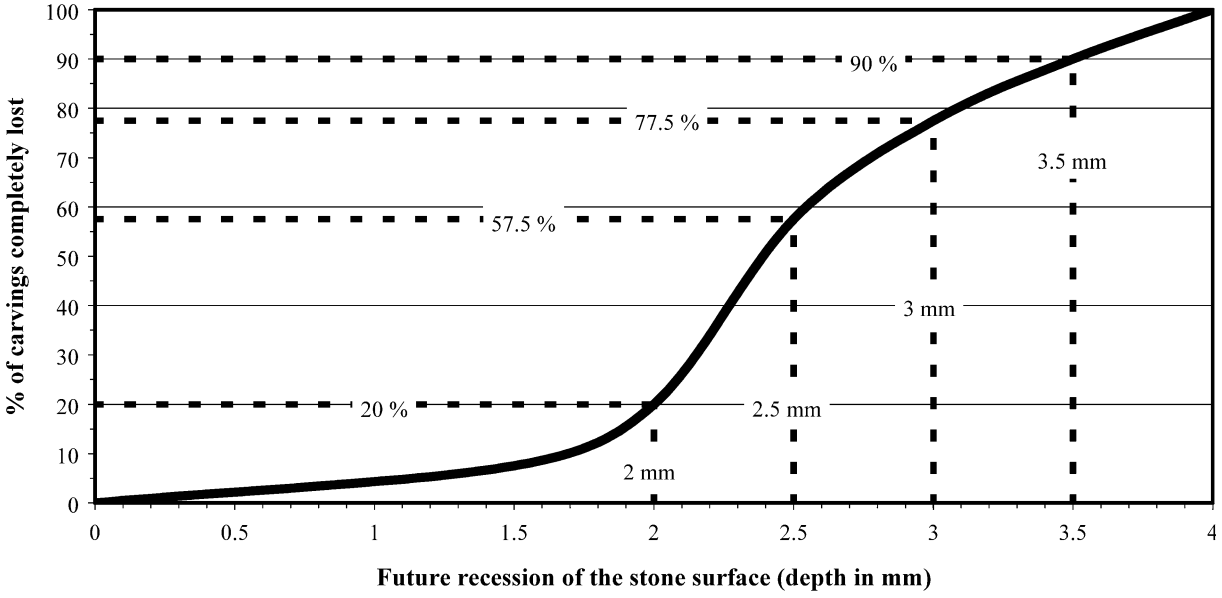

Fig. 26
Risk prognosis derived from profile measurements

References

Fitzner B, Heinrichs K (2002) Damage diagnosis on stone monuments—weathering forms, damage categories and damage indices. In: Prikryl R, Viles H (eds) Understanding and managing stone decay. Proceedings of the international conference "Stone weathering and atmospheric pollution network" (SWAPNET 2001). Charles University, Prague, Karolinum Press, pp 11–56

Fitzner B, Heinrichs K, Kownatzki R (1995) Weathering forms—classification and mapping. Denkmalpflege und Naturwissenschaft, Natursteinkonservierung I. Ernst & Sohn, Berlin, pp 41–88

Fitzner B, Heinrichs K, La Bouchardiere D (2002) Damage index for stone monuments. In: Galan E, Zezza F (eds) Protection and conservation of the cultural heritage of the Mediterranean cities. Proceedings of the 5th international symposium on the conservation of monuments in the Mediterranean basin, Sevilla, Spain, 5–8 April 2000, Swets & Zeitlinger, Lisse / Netherlands, pp 315–326

Kim SJ (ed) (2002) Proceedings of the international symposium on the conservation of the Bangudae Petroglyph, Stone Conservation Science Laboratory, Ulsan City

Pettijohn FJ, Potter PE, Siever R (1987) Sand and sandstone, 2nd edn. Springer, Berlin Heidelberg New York